State-to-State Behavior in the Neutral Dissociation of O_2 Far beyond the Ionization Threshold

M. Ukai,[1] S. Machida,[1] K. Kameta,[1] M. Kitajima,[1] N. Kouchi,[1] Y. Hatano,[1] and K. Ito[2]

[1]*Department of Chemistry, Tokyo Institute of Technology, Tokyo 152, Japan*

[2]*Photon Factory, National Laboratory for High Energy Physics, Ibaraki 305, Japan*

(Received 22 November 1993)

The two-dimensional yield spectrum of fluorescence radiation from excited O atoms produced in the neutral photodissociation of O_2 is measured as a function of both excitation photon wavelength of 50–62 nm (24.8–20 eV photon energy) and fluorescence wavelength of 80–140 nm. State-to-state neutral dissociation pathway of the Rydberg states converging onto $O_2^+(c\,^4\Sigma_u^-)$, $v' = 1$ into the $O(ns\,^3S) + O(^1D)$ dissociation limit is revealed, where the principal quantum numbers of the Rydberg orbitals are conserved into those of excited O atoms.

PACS numbers: 33.20.Ni, 33.50.–j, 33.80.Gj, 39.10.+j

Neutral dissociation of an excited molecule in the energy region far beyond its ionization potential (IP) is one of the unrevealed mysteries. A neutral excited molecule AB^{**} lying above its IP, i.e., in superexcited state, is embedded in two kinds of continuum states. One is the ionization continuum and another is the continuum of nuclear motion. As the result of rearrangement of electronic configuration due to electron correlation, AB^{**} will decay nonradiatively by the spontaneous electron emission [autoionization (1)], or by the neutral dissociation (ND) via nonadiabatic transition (2) [1,2], i.e.,

$$AB^{**} \rightarrow AB^+ + e^- \quad (1)$$

$$\hookrightarrow A + B. \quad (2)$$

As the primary concept, the competition between (1) and (2) is generally accepted for the decay of AB^{**} lying close to IP [1].

Recent observations of the process (1) for high-lying AB^{**} excited by photoabsorption have provided advanced aspects on photon-induced ionic decay processes [3–6]. Although the behavior of ND near IP was shown by measuring the absolute photoionization quantum yield [7], studies in the energy region about, e.g., twice of IP have been discouraging. This is due to the experimental difficulties in observing the process (2) and, furthermore, to the general idea of the process as "the minor decay channel following superexcitation (3b) which is minor in total photoabsorption [(3a) + (3b)]," [1] for

$$AB + h\nu \rightarrow AB^+ + e^- \quad (3a)$$

$$\hookrightarrow AB^{**}. \quad (3b)$$

Only preliminary data and analyses have been given in this region for ND of simple molecules such as O_2 [8,9]. However, the complex electron correlation in populating and destructing AB^{**} is purely reflected in ND [10], which is not the case for the ionic channel [(1) + (3a)] because of the major contribution from direct one-electron ionization (3a) involved [3]. Thus, new aspects of correlation effects in a molecular field can be provided by a detailed study of ND far beyond the IP, i.e., by showing *how, to what extent,* or *with what selectivity or preference* ND occurs.

In this Letter a detailed measurement of photon-induced ND of O_2 far beyond its IP (12.07 eV) is shown. We reveal here a "location map" or "bird's-eye view" of the ND feature by measuring the yield spectrum of fluorescence radiation (FES, fluorescence excitation spectrum) emitted from excited O^* atoms as a function of both excitation photon wavelength λ_{ex} for $50 \leq \lambda_{ex} \leq 62$ nm (24.8–20 eV photon energy) and fluorescence wavelength λ_f for $80 \leq \lambda_f \leq 140$ nm, i.e.,

$$O_2 + h\nu(\lambda_{ex}) \rightarrow O_2^{**}\,(\text{superexcited state})$$

$$\hookrightarrow O + O^*$$

$$\hookrightarrow O + h\nu(\lambda_f).$$

We present the superexcited states having repulsive and bound potential curves decaying into ND. It has been supposed that the multichannel crossing between the states correlating with various ND channels causes wide distribution in the final fragments [8]. However, a "two-dimensional location map" shows the striking behavior of ND far beyond the IP, i.e., a highly selective or even "state-to-state ND" of the $(c\,^4\Sigma_u^-)ns\sigma_g$ and $nd\pi_g$, $v' = 1$ Rydberg states.

The experiment was performed using synchrotron radiation (SR) from a 2.5 GeV positron storage ring at the Photon Factory. The SR from a 3 m normal incidence monochromator was intersected with O_2 gas in a cell. The flux of SR transmitted through the cell (typically 1×10^{11} photons/s at 20 eV) was monitored using a photomultiplier behind a glass window coated with sodium-salicylate. FES was measured with steps of 0.05 nm in λ_{ex} with the nominal band pass of SR of 0.13 nm (45 meV resolution at 20 eV). The fluorescence radiation emitted from the gas was dispersed using a holographic 1200 lines/mm grating with a curvature radius 20 cm at a dispersion angle 64°. The dispersed image of fluorescence spectrum was obtained using a continuous resistive-anode-type position sensitive detector behind a microchannel plate (MCP) coated with CsI

0031-9007/95/74(2)/239(4)$06.00

[11]. The fluorescence spectra were not corrected for the detection efficiency, which was known to be a smoothly decreasing function by a 25% reduction, with λ_f from 90 to 130 nm. The absolute wavelength of SR was calibrated for the neutral O_2^{**} levels in $86 \leq \lambda_{ex} \leq 98$ nm [12]. Two-stage differential pumping between the gas cell and the secondary monochromator was employed to avoid the attenuation of fluorescence by a background gas. Collisional quenching or redistribution of O^* atoms was carefully determined to be negligible. This allowed us to correct the FES only for the SR photon flux and the sample gas pressure in the cell.

The FES of undispersed fluorescence for $150 \leq \lambda_f \leq 180$ nm transmitted through a laser-induced fluorescence spectroscopy (LIF) window was also obtained using a CsI coated MCP [2,10].

Figure 1 shows the two-dimensional FES emitted from dissociatively excited neutral O atoms as a function of λ_{ex} for $50 \leq \lambda_{ex} \leq 60$ nm (photon energy 24.8–20 eV). In this region of λ_{ex}, atomic ions are not energetically accessible as the partners of the dissociative, ionization, and excitation for the O^* atoms. Each of the horizontal line structures in Fig. 1 presents the partial fluorescence yield from individual O^* atoms produced in the ND of O_2^{**}. The identified O I radiation lines are listed in Table I. It is also shown that the molecular fluorescence from the parent ion is absent. The smooth variation of the fluorescence yields shows the dissociation of repulsive O_2^{**}. However, the potential curves for these repulsive O_2^{**} are not identified. Possible repulsive O_2^{**} states are the Rydberg states with the repulsive ions cores of correlation states [13], such as those shown in Fig. 2.

As well as the smooth variation, the discrete structures of fluorescence yields are also observed at λ_{ex} to excite well-defined vibronic levels of $ns\sigma_g$ and $nd\pi_g$ ($n \geq 3$) Rydberg series converging onto $O_2^+(c\,^4\Sigma_u^-, v = 0$ and 1) ions [14,15]. Although some O I lines overlap with others due to the limited resolution of about 2 nm, there are observed well-identified resonance structures of certain O I lines among the overlapping manifolds. However, the behavior of enhanced fluorescence yields is different at λ_{ex} to excite $v' = 0$ or $v' = 1$ levels. The yields of several O I lines at λ_{ex} for $v' = 0$ are enhanced simultaneously, which is ascribed to the partitioning in a multichannel predissociation. By contrast, at λ_{ex} for $v' = 1$ levels of each n (principal quantum number) states of $O_2^{**}(c\,^4\Sigma_u^- ns\sigma_g$ or $nd\pi_g)$, the production of $O(ns\,^3S)$ ($n \geq 3$) atoms is emphasized strongly and selectively [16], where the n quantum number is conserved,

$$O_2^{**}(c\,^4\Sigma_u^- ns\sigma_g \text{ or } nd\pi_g) \rightarrow O(ns\,^3S) + O. \quad (4)$$

The fluorescence spectra at λ_{ex} for $c\,^4\Sigma_u^- ns\sigma_g$, $v' = 1$ ($3 \leq n \leq 7$) in Fig. 3 clearly show this behavior. This striking behavior is evidence of the state-to-state selective

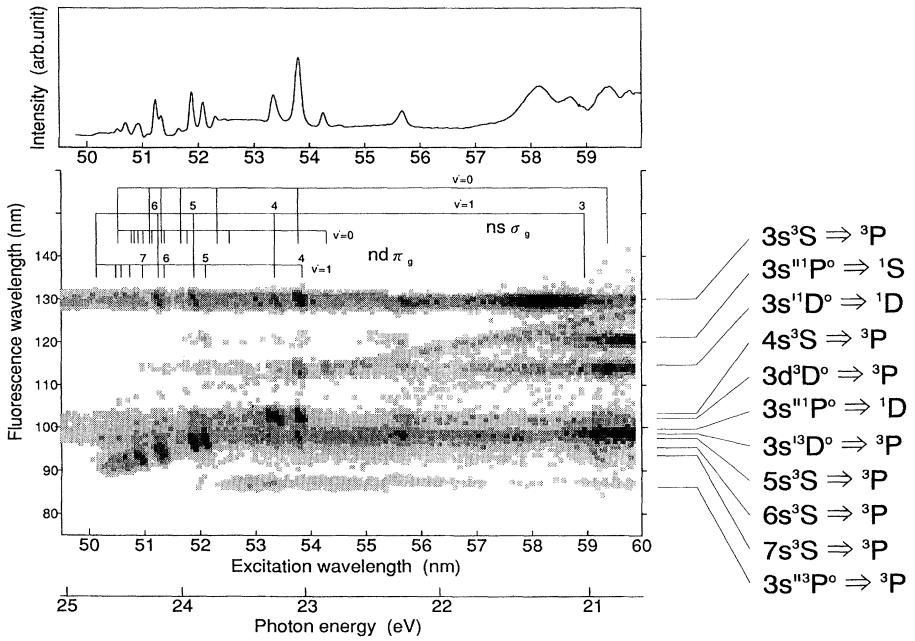

FIG. 1. Two-dimensional yield spectrum of the fluorescence radiation (two-dimensional FES) emitted from neutral O^* atoms produced in the neutral photodissociation of O_2^{**} as a function of both the excitation wavelength for $50 \leq \lambda_{ex} \leq 60$ nm and fluorescence wavelength for $80 \leq \lambda_f \leq 140$ nm (lower panel). The yields presented by the grey rectangle plots increase from white to black linearly with 8 steps of the color. Horizontal line structures present the partial fluorescence yields of O I radiation lines (see also Table I). Yield spectrum (FES) of nondispersed fluorescence for $105 \leq \lambda_f \leq 180$ nm (upper panel) is shown together.

TABLE I. Identified O I fluorescence radiation lines and dissociation products. Notice that all the fluorescence appears at the lowest dissociation energy limit of $O(n\ell) + O(^3P)$ [8].

Fluorescence wavelength (nm)	Transitions	Dissociation energy limits		
		Dissociation products	Energy (eV)	Wavelength (nm)
130.4	$3s\,^3S \rightarrow {}^3P$	$O(3s\,^3S) + O(^3P)$	14.6	84.7
121.8	$3s''\,^1P^0 \rightarrow {}^1D$	$O(3s''\,^1P^0) + O(^3P)$	19.5	63.6
115.2	$3s'\,^1D^0 \rightarrow {}^1D$	$O(3s'\,^1D^0) + O(^3P)$	17.8	69.4
103.9	$4s\,^3S \rightarrow {}^3P$	$O(4s\,^3S) + O(^3P)$	17.0	72.7
102.7	$3d\,^3D^0 \rightarrow {}^3P$	$O(3d\,^3D^0) + O(^3P)$	17.2	72.1
99.9	$3s''\,^1P^0 \rightarrow {}^1S$	$O(3s''\,^1P^0) + O(^3P)$	19.5	63.6
99.1	$3s'\,^3D^0 \rightarrow {}^3P$	$O(3s'\,^3D^0) + O(^3P)$	17.7	70.2
97.6	$5s\,^3S \rightarrow {}^3P$	$O(5s\,^3S) + O(^3P)$	17.8	69.6
95.2	$6s\,^3S \rightarrow {}^3P$	$O(6s\,^3S) + O(^3P)$	18.2	68.3
94.0	$7s\,^3S \rightarrow {}^3P$	$O(7s\,^3S) + O(^3P)$	18.3	67.6

ND being against such general understanding in this region that the multistep predissociation populates various fragments at the ND limits [1]. It should also be noticed that the enhanced yield in the $O(3s\,^3S \rightarrow {}^3P)$ line at λ_{ex} for $c\,^4\Sigma_u^- 3s\sigma_g$, $v' = 1$ is not so strong as compared with other $ns\sigma_g$ levels but followed by another structure around 58 nm. The latter enhancement observed in our recent work was interpreted as the direct ND of O_2^{**} vertically populated on the $c\,^4\Sigma_u^- 3s\sigma_g$ repulsive wall into the $O(3s\,^3S) + O(^1D)$ limit [8]. The present state-to-state behavior and the direct ND [11] are explained without contradiction by the fast ND on Rydberg-state potential curves.

Tanaka and Yoshimine [17] showed the $O_2^+(c\,^4\Sigma_u^-)$ potential curve adiabatically converging to $O^+(^4S) + O(^1D)$. A quasibound potential minimum only supports the $v' = 0$ and 1 levels of the ion. By the addition of an $ns\sigma_g$ Rydberg electron to this ion both around the Franck-Condon (FC) region and at dissociation limit, one can draw the $O_2^{**}(c\,^4\Sigma_u^- ns\sigma_g)$ potential curve connected to $O(ns\,^3S) + O(^1D)$ [11]. They also calculated the tunneling-dissociation rates of 10^{11} s^{-1} for the $v' = 1$ level of $c\,^4\Sigma_u^-$ ion, which was three decades greater than that for $v' = 0$ [17]. Analogously, after the tunneling through the barrier of the quasibound $v' = 1$ level, O_2^{**}

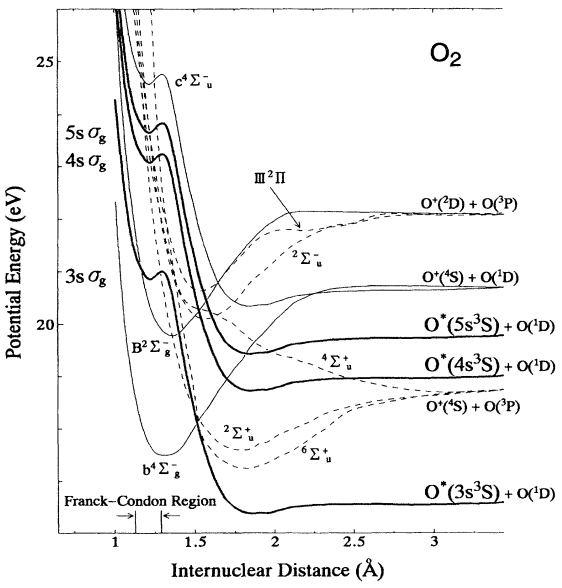

FIG. 2. Potential energy curves for $O_2^{**}(c\,^4\Sigma_u^-)ns\sigma_g$ ($n = 3 - 5$) (—), nominal one-electron states (—), and correlation states (––) [13]. $O_2^{**}(c\,^4\Sigma_u^-)ns\sigma_g$ curves (diabatic presentation to radial coupling) are estimated considering ion-core potential curve [16], Rydberg energy levels [14], and ND energy limits (see text).

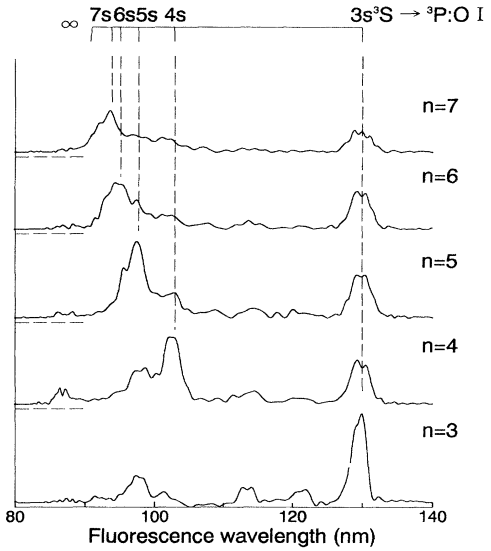

FIG. 3. Fluorescence spectra of O I obtained at λ_{ex} to excite $c\,^4\Sigma_u^- ns\sigma_g$, $v' = 1$ ($3 \leq n \leq 7$) from two-dimensional FES in Fig. 1. The largest fluorescence yields at λ_f of O I ($ns\,^3S \rightarrow {}^3P$) are originated from the state-to-state neutral dissociation of $O_2^{**}(c\,^4\Sigma_u^- ns\sigma_g)$, $v' = 1$ with the identical n.

populated on the repulsive wall undergoes fast ND into $O(ns\,^3S) + O(^1D)$ limit, which dominates the ND under the competition with autoionization. This is obvious at λ_{ex} for the $n = 4 - 7$ levels (Figs. 1 and 3). The absence of the selective enhancement at any $v' = 0$ level, however, suggests that the tunneling is no more important in the ND of a $v' = 0$ level. Since the $c\,^4\Sigma_u^-$, $v' = 0$ ion predissociates into $^{2,4,6}\Sigma_u^-$ and $^2\Sigma_u^+$ repulsive states around the quasibound region [18], the similar interaction among the ion-core configurations of the O_2^{**} Rydberg state is naturally important (Fig. 3), which initiates multistep predissociation. Similar discussion is possible for $nd\pi_g$, $v' = 0$ and 1 states.

Previous photoionization studies showed the largest amplitude of superexcitation (3b) onto $c\,^4\Sigma_u^- 3s\sigma_g$, $v' = 0$ and 1 among the $ns\sigma_g$ Rydberg series [4–6]. It is clear, however, that the largest enhancement of $O_2^{**}(c\,^4\Sigma_u^- 3s\sigma_g) \rightarrow O(3s\,^4S) + O$ is not obtained at λ_{ex} for $v' = 0$ and 1 in the present FES. This gives the aspect of tunneling ND of O_2^{**} under the competition with autoionization and other predissociation around the FC region. The strong configuration interaction in the $c\,^4\Sigma_u^-$ ion core around the quasibound region was exemplified by the enhanced dipole transition moment $\langle c\,^4\Sigma_u^- | r | b\,^4\Sigma_g^+ \rangle$ [17]. This predicts enhanced probabilities of nonradiative transitions in O_2^{**}, such as the Coster-Kronig-type autoionization into $b\,^4\Sigma_g^+$ or the $B\,^2\Sigma_g^+$ ion [4–6], which is largest for $n = 3$. Also the $c\,^4\Sigma_u^- 3s\sigma_g(^3\Sigma_u^-)$ potential curve intersects that of $B\,^4\Sigma_g^+$ around the quasibound region [11], implying crossing with a number of $B\,^4\Sigma_g^+ np\sigma_u(^3\Sigma_u^-)$ states and enhanced predissociation into these Rydberg states. These two kinds of nonradiative transitions reduce the tunneling dissociation of $c\,^4\Sigma_u^- 3s\sigma_g$, $v' = 1$ but pronounce the $O(3s\,^3S \rightarrow {}^3P)$ yield at λ_{ex} for the repulsive wall. However, none of $ns\sigma_g$ and $nd\pi_g$ ($n \geq 4$) crosses with them. Significantly reduced rates for autoionization and predissociation of the $ns\sigma_g$ and $nd\pi_g$ ($n \geq 4$), $v' = 1$ Rydberg states increases the available possibilities of tunneling to result in the state-to-state dissociation.

This work was performed under the approval of the Photon Factory Program Advisory Committee (No. 92-156). Financial support from the Grant-in-Aid for Scientific Research of the Ministry of Education, Science and Culture, Japan is acknowledged. The authors thank Dr. T. Hayaishi for collaboration.

[1] I. Nenner and J. A. Beswick, in *Handbook on Synchrotron Radiation,* edited by G. V. Marr (North Holland, Amsterdam, 1987), Vol. 2, p. 355.

[2] M. Ukai, K. Kameta, N. Kouchi, K. Nagano, Y. Hatano, and K. Tanaka, J. Chem. Phys. **97**, 2835 (1992).

[3] J. W. Gallagher, C. E. Brion, J. A. R. Samson, and P. W. Langhoff, J. Phys. Chem. Ref. Data **17**, 9 (1988).

[4] P. Morin, I. Nenner, M. Y. Adam, M. J. Hubin-Franskin, J. Delwiche, H. Lefebvre-Brion, and A. Giusti-Suzor, Chem. Phys. Lett. **92**, 609 (1982).

[5] M. Ukai, A. Kimura, S. Arai, P. Lablanquie, K. Ito, and A. Yagishita, Chem. Phys. Lett. **135**, 51 (1987).

[6] A. A. Cafolla, T. Reddish, A. A. Wills, and J. Comer, J. Phys. B **23**, 1433 (1990).

[7] D. M. P. Holland, D. A. Shaw, S. M. McSweeny, M. A. MacDonald, A. Hopkirk, and M. A. Hayes, Chem. Phys. **173**, 315 (1993).

[8] L. C. Lee, R. W. Carlson, D. L. Judge, and M. Ogawa, J. Chem. Phys. **61**, 3261 (1974).

[9] K. Codling, L. J. Frasinski, and K. J. Randall, J. Phys. B **18**, L251 (1985).

[10] M. Ukai, K. Kameta, N. Kouchi, Y. Hatano, and K. Tanaka, Phys. Rev. A **46**, 7019 (1992).

[11] M. Ukai, N. Kouchi, K. Kameta, N. Terazawa, Y. Chikahiro, Y. Hatano, and K. Tanaka, Chem. Phys. Lett. **195**, 298 (1992).

[12] K. Yoshino and Y. Tanaka, J. Chem. Phys. **48**, 4859 (1968).

[13] N. H. F. Beebe, E. W. Thulstrup, and A. Andersen, J. Chem. Phys. **64**, 2080 (1976).

[14] K. Codling and R. P. Madden, J. Chem. Phys. **42**, 3935 (1965).

[15] The assignment of the $(c\,^4\Sigma_u^-)nd\pi_g$ Rydberg series is employed tentatively. This still needs discussion and further evaluation of quantum defects [see Ref. [14] and also E. Lindholm, Ark. Phys. **40**, 117 (1968); P. H. Krupenie, J. Phys. Chem. Ref. Data **1**, 423 (1972)]. However, in the assignment of molecular Rydberg states, the present result suggests the importance of the general feature of adiabatic potential curves and correlating dissociation limits..

[16] We do not discuss the weak enhancement of O I $(3s\,^3S \rightarrow {}^3P)$ at λ_{ex} for different n states, the origin of which can be attributed to cascade processes.

[17] K. Tanaka and M. Yoshimine, J. Chem. Phys. **70**, 1626 (1979).

[18] M. Richard-Viard, O. Dutuit, M. Lavollée, T. Govers, P. M. Guyon, and J. Durup, J. Chem. Phys. **82**, 4054 (1985); M. Richard-Viard, O. Dutuit, M. Ait-Kaci, P. M. Guyon, and J. Durup, J. Phys. B **20**, 2247 (1987).